Available online at www.ijournalse.org

Emerging Science Journal

(ISSN: 2610-9182)

Vol. 9, No. 5, October, 2025

Corrosion Performance of a Novel Aluminium 6061-Sea Sand Composite Under Electrochemical Method

Eko Surojo [1*], Teguh Triyono [1], Hammar Ilham Akbar [2], Ganjar Pramudi [2], Triyono [1], Wijang W. Raharjo [1], Raiddin Muhamad Agiel [1], Faishal M. Majid [1], Harjo Seputro [3], Ilham Habibi [4]

[1] *Department of Mechanical Engineering, Faculty Engineering, Universitas Sebelas Maret, 57126, Surakarta, Indonesia.*

[2] *Department of Mechanical Engineering, Vocational School, Universitas Sebelas Maret, 57126, Surakarta, Indonesia.*

[3] *Department of Mechanical Engineering, Universitas 17 Agustus 1945 Surabaya, 60118, Surabaya, Indonesia.*

[4] *Department of Mechanical Engineering, Universitas Muhammadiyah Magelang, 59124, Magelang, Indonesia.*

Abstract

The need for lightweight materials is increasing from year to year. In its application, lightweight and strong materials also need to be corrosion resistant. Corrosion resistance is an important property in automotive, especially in high humidity areas. Al6061-Sea sand material is a novel material that meets the mechanical standards required in the automotive sector. A previous study of Al 6061-sea sand conducted the mechanical properties of the composite. This current research focuses on the development of Al 6061 material with variations in weight fraction of sea sand reinforcement against the corrosion rate under the potentiodynamic method to determine the corrosion resistance of the composite material. The composite fabrication uses the electroless coating method on sea sand and the stir casting method with a melting temperature of 750°C. The agitation process used a four-bladed impeller for 10 minutes at 600 rpm with a stirring depth of ½ of the height of the molten metal. The tests include density testing, microstructure observation, and corrosion rate under the potentiodynamic method using an electrochemical potentiostat. The test result obtained the lowest corrosion rate results in 2% wt sea sand with a corrosion rate of 0.61875 mmpy. The increase in corrosion rate value is directly proportional to the addition of the weight fraction of sea sand.

Keywords:

Aluminium Matrix Composite;
Potentiodynamic;
Electrochemical Potentiostat;
Corrosion Rate.

Article History:

Received: 24 December 2024
Revised: 04 July 2025
Accepted: 17 July 2025
Published: 01 October 2025

1- Introduction

The first Aluminum Matrix Composite (AMC) is an intriguing material, as it combines high strength and stiffness with low density. Other advantages include high temperature strength, good resistance to thermal fatigue, good shock resistance, high thermal conductivity, and low coefficient of thermal expansion [1]. The composite manufacturing method was proven to significantly matter in determining the physical and mechanical characteristics of the composite material, microstructure, and interfacial bonding between the matrix and reinforcement [2]. Stir casting is one of the composite fabrication processes used to produce AMC. This process involves the use of a stirrer to mix the reinforcement into the matrix material. There are certain drawbacks to the stir casting method, such as the wettability between the reinforcing particles and the matrix metal, that will affect the interfacial bonding between the particles, especially the

---

* **CONTACT**: ekosurojo@staff.uns.ac.id

DOI: http://dx.doi.org/10.28991/ESJ-2025-09-05-012

wettability. Good quality interfacial bonding occurs when the reinforcing particles can be perfectly wetted by the matrix. Wettability is the required condition for the formation of bonds between the matrix and the reinforcement so that the composite can distribute the loads without experiencing breakage [3]. One of the approaches to increase wettability is through the use of the electroless coating method [4]. Electroless coating can effectively improve the wettability between the reinforcing particles and the aluminum matrix.

Aluminum alloy 6061 (Al6061) is a popular material that continues to be developed to support the advancement of the automotive and aerospace industries. The advantages of Al6061 include good machinability, weldability, and heat treatability. However, environmental corrosion resistance is a major challenge that must be overcome [5]. Corrosion in aluminum matrix composites (AMC) is often initiated by weak bonds between the reinforcing particles and the matrix or by cracks in the reinforcing particles, which then cause pitting. The level of corrosion in AMC is greatly influenced by factors such as the type, volume, size, and distribution of the reinforcing particles used [6]. The influence of mass fraction on the corrosion resistance of aluminum composites can vary, depending on the specific composition and testing conditions. Furthermore, previous research has shown that composites with an increased mass fraction of reinforcing material (MWCNT) enhance the corrosion resistance of the composite. A composite with a mass fraction of 1.75% wt has a corrosion rate value of 438.880 mm/yr, which is lower than the corrosion rate of pure AA5083, which is 472.836 mm/yr [7].

The mechanical properties of Al 6061-sea sand have been tested in previous studies; the results obtained by increasing the weight fraction of sea sand will increase its mechanical properties. In order to obtain superior AMC material, further research on corrosion resistance is needed. As is known, the corrosion rate is a considered parameter when selecting materials for construction use, industrial equipment, and daily needs, so this study focuses on the development of Al 6061 material with an alloy of Mg 0.802% wt - Si 0.43% wt, reinforced with sea sand at various fractions of 2% wt, 4% wt, and 6% wt, to assess the corrosion rate using the potentiodynamic testing method, aiming to determine the corrosion resistance of the composite material. This study aims to investigate the effect of increasing the number of reinforcing particles on the corrosion rate of the novel Al6061-sea sand composite.

2- Literature Review and Research Objective

Aluminum Matrix Composites (AMC) have replaced conventional engineered materials due to their superior properties, lightweight, and good mechanical strength. Corrosion behavior in AMC is an important parameter in assessing the potential application of composites as alternative material. Investigations regarding corrosion behavior have been reported recently. The secondary phase, which is the main reinforcement element in the fabrication of AMC, is the preferred location at the time of corrosion formation. Reinforcement particles can interact electrochemically, chemically, or physically with matrix metals, which can lead to accelerated corrosion [8]. In general, aluminum metal alloys have better corrosion resistance compared to AMC. This is because aluminum alloy contains an oxide layer on its surface that, when exposed to the environment, performs a chemical reaction and creates a passive layer that can protect aluminum alloy against corrosion. However, in AMC, the passive layer on aluminum alloys is damaged due to the addition of reinforcing particles that make it susceptible to corrosion [9].

The effect of the addition of reinforcement particles on the corrosion resistance behavior of AMC has been carried out in several studies. An experimental study of the corrosion behavior of AA1100 metal composite reinforced with B_4 C ceramic particles has been conducted by Han et al. Potentiodynamic corrosion studies were performed on the Al-B_4 C metal composite in open water and argon-deaerated conditions. It is known that increasing the volume fraction of B_4 C causes a significant decrease in corrosion resistance. The increased volume of B4C in the composite increases the discontinuity in the oxide layer of the protective surface, making the composite more susceptible to chloride ions and resulting in poor potential for corrosion resistance [10].

Poor corrosion behavior in AMC results in a decrease in the mechanical properties of the composite, which affects the performance of the material. The addition of ceramic particles to AMC leads to the durability properties of aluminum composites decreasing. Das et al. studied the influence of ceramic reinforcement particle size on the corrosion behavior of AMC. Aluminum metal composites reinforced by Cu/Zircon sand with particle sizes of 65, 90, and 135 mm are made using the stir casting method. The results showed that the corrosion rate in AMC increased along with the increase in the size of the reinforcing particles. The increasing corrosion rate is associated with smaller particle sizes that are able to stop pit growth [11]. In addition, when particle size increases, interface cavities emerge due to the increasing contact surface area. The formation of cavities at the interface results in a higher rate of corrosion [12].

The fabrication process in the AMC, the dispersion of reinforcement particles in a uniform matrix, and porosity are important parameters that need to be considered. The selection of the right fabrication method can affect the corrosion behavior of AMC materials. The presence of porosity can be the initiation of an increase in the anode current rate, which has the potential to accelerate the corrosion rate in AMC [13]. To overcome these problems, it is necessary to select the right fabrication method and operating parameter. Cheng et al. investigated the corrosion behavior of Al7075 reinforced by SiC particles with a potentiodynamic polarization measurement. Al7075-SiC composite is made by the multi-layer spray deposition fabrication method and subsequently extruded. The results of potentiodynamic measurements in the cathodic process show that nonconductive SiC ceramic particles cannot act as active cathodes, so the cathode current will be reduced. The anodic process shows a lower AMC dissolution rate, which can also be interpreted by minimizing the corrosion area. The AMC fabrication process using multi-layer spray deposition has been proven to be able to increase corrosion resistance, because this method can make a denser composite than ordinary AMC. In addition, SiC particles play an inert role; production defects and internal stresses are minimized so that the corrosion resistance of AMC can be improved [14].

Alaneme et al. [15] investigated the corrosion behavior in Al6063 composite reinforced with Al2O3 by the stir casting fabrication method. Corrosion characterization was carried out by immersing the composite in a solution of NaCl (pH 7.4), H_2SO_4 (pH 0.9), and NaOH (pH 12.7); then mass loss and corrosion rate were measured in a span of 2 days for intervals of 40, 29, and 45 days. The corrosion rate was obtained to increase along with the increase in Wt% of the reinforcement. This can be caused by the segregation of reinforcement particles in the matrix, which is common in cast fabrication methods. Particle segregation leads to the formation of holes that facilitate corrosion [16]. In addition, corrosion initiation can occur at the poor interface bonding of the matrix reinforcement particles [17].

Research on corrosion rates in AMC reinforced by natural materials is still very much needed to be developed. Natural materials are currently widely developed as alloys to develop metal composite materials. The selection of natural materials is based on economic costs and high ceramic content, which can increase mechanical strength. Therefore, it is necessary to investigate the corrosion behavior of AMC reinforced by natural materials. Aliyu et al. have investigated the corrosion behavior of AMC reinforced by natural materials. Sugar palm ash reinforced LM26 matrix metal with wt% variation. Corrosion characterization is carried out by immersing composites in HCL solution. The corrosion rate increased along with the increase in the reinforcement content [18]. The addition of reinforcement damages the thin layer of oxide contained in the aluminum matrix, making it susceptible to corrosiveness [19]. Acid solution dissolves reinforcing particles during corrosion tests. Furthermore, intermetallic compounds create galvanic cells in acid solutions, resulting in a growth of corrosion rates in composites [20].

The integration of graphene into aluminum matrix composites (AMC) by powder metallurgy has been shown to improve the mechanical properties of the material, although at the expense of reduced corrosion resistance. The potential of graphene as a reinforcement in AMC is supported by its superior mechanical properties. A study conducted by Yang et al. showed that the addition of graphene at a concentration of 0.3 wt% resulted in optimal tensile performance. This phenomenon was attributed to the increase in the interfacial area between aluminum and graphene, which facilitated efficient load transfer. In contrast, at a concentration of 0.5 wt%, graphene agglomeration occurred at the grain boundaries, which triggered crack formation and reduced the ultimate tensile strength (UTS) values. In addition, the addition of graphene was correlated with increased susceptibility to corrosion. The micro galvanic corrosion mechanism occurs due to the contact between graphene and aluminum in an NaCl solution environment, with aluminum acting as the anode and graphene as the cathode. This process results in the oxidation of aluminum to Al^{3+}, which accelerates the corrosion rate. Tafel diagram analysis shows a shift in the corrosion potential (E_{corr}) in a negative direction and an increase in the corrosion current density (i_{corr}) as the graphene concentration increases [21]. Higher i_{corr} values indicate that the corrosion rate occurs faster [22].

Potentiodynamic tests were conducted by Prabakaran et al. to evaluate the corrosion rate of aluminum 6063 composites reinforced with SiC particles and tungsten disulfide. The analysis results showed a significant decrease in corrosion current density (icorr) after the addition of reinforcing particles. This increase in corrosion resistance is attributed to the formation of a good bond between the aluminum matrix and the reinforcing particles, resulting in an increase in interface quality compared to unreinforced Al6063 [23]. In their research, Patel et al. showed that the addition of Si_3N_4 to the Al6063 matrix resulted in a significant increase in corrosion resistance compared to unreinforced Al6063. With the addition of Si_3N_4 at 5 wt% and 10 wt%, the corrosion rate of Al6063 was successfully reduced from 43.61 mmpy to 6.91 mmpy and 1.72 mmpy, respectively. This significant decrease in corrosion rate is attributed to the role of the reinforcing particles as a barrier to the diffusion of corrosive ions and the reduction of the contact area between the Al6063 matrix and the corrosive environment (NaCl solution) [24].

The electrolyte fluid used in potentiodynamic testing has a significant effect on the corrosion rate of iron (Fe)-based aluminum matrix composite (AMC) materials. A study conducted by Cui et al. investigated the effects of different immersion solutions on potentiodynamic testing, namely NaCl, H_2SO_4, and NaOH. The measurement results showed corrosion rates of 0.0449 mmpy, 0.355 mmpy, and 0.90 mmpy, respectively. The formation of a passive layer on the AMC surface during the immersion process was shown to correlate with the level of corrosion resistance. X-ray photoelectron spectroscopy (XPS) characterization was performed to identify the chemical composition of the passive layer formed on each sample [25].

Based on literature studies, the use of the stir casting method is the most economical and conventional way to produce AMC. However, the stir casting method has several drawbacks, including uneven particle distribution and imperfect bonding between particles and matrix metal during the casting process. The imperfect interface bond between the matrix and the reinforcement causes the growth of galvanic cells that can dissolve the Al matrix, resulting in decreased corrosion resistance [26]. To overcome this problem, it is necessary to make modifications in the AMC fabrication method by applying a coating to the reinforcement particles to improve the interface bonding. To achieve good interface bonding strength, the wettability of reinforcement particles with molten aluminum metal is an important factor in composite properties. Coating of the reinforcement particles can increase wettability by decreasing the surface tension and interface energy of the matrix and reinforcement [27].

Zakaulla et al. [28] investigated the effect of reinforcing particle coating on the corrosion behavior of Al6061-SiC composites. SiC ceramic particles were coated with Cu using the electroless coating method to improve interfacial bonding. Al6061-SiC composite is manufactured using the stir casting technique, then characterized by a corrosion test by immersion in NaCl solution for 72, 144, 216, 288, and 360 h. The results show that the coating of particles with Cu can improve wettability so that the bonding of the matrix interface and reinforcement particles can be improved. However, particle coating with Cu lowers the corrosion resistance of the composite. This is because Cu is a conductor material, increasing the cathode ratio around the SiC reinforcement particle, which easily leaves an electron charge, and corrosion occurs in the SiC particle area [28].

Growing awareness of the importance of sustainability, researchers are exploring ways to make Aluminum Matrix Composites (AMCs) more affordable and environmentally friendly by using natural materials that are easy to obtain. Based on literature studies, this study uses the stir casting fabrication method, which is the most economical method and straightforward to implement on an industrial scale. Sea sand was utilized as a reinforcement element in AMC because it is an easy-to-obtain material and has a high ceramic content. To improve corrosion resistance, the reinforcement particles are coated with Al and Mg to improve the wettability of the reinforcement particles and aluminum matrix. Good wettability can improve the interface bonding, resulting in improved corrosion resistance. The selection of Al and Mg alloys as reinforcing coatings can react to generate the spinel phase of $Al_2 MgO_4$. $Al_2 MgO_4$ spindles can produce a protective layer when exposed to corrosive agents [29].

3- Materials and Methods

3-1- Materials

In the composite fabrication process, this research utilizes several materials, including Alloy 6061-type purchased from UD Sutindo Sejahtera, Surabaya, East Java. The chemical composition data of the aluminum alloy series 6061 presented in Table 1. The sea sand used in this research was from Samas, located in Bantul, Yogyakarta, Indonesia. The following data of the chemical composition of sea sand is presented in Table 2. Sea sand is a natural material that is easy to find, especially in an archipelagic country like Indonesia. The sea sand used in this article comes from Samas Beach, which has a chemical composition that includes SiO_2 , $Fe_2 O_3$, and other components. Sea sand also shows properties such as a density of 2.62 g/cm³, a modulus of elasticity of 124.28 (GPA), and a hardness of 6-6.5 (Mohs) [30].

Table 1. Chemical composition of Aluminium

Component	Amount (Wt%)
Aluminum	96.85
Magnesium	0.9
Silicon	0.7
Iron	0.6
Copper	0.30
Zinc	0.20
Manganese	0.05
Other Components	0.40

Table 2. Chemical composition of Samas sea sand [31]

Component	Amount (Wt%)
SiO_2	51.2
Fe_2O_3	48.2
Other Components	0.6

3-2- Composite Fabrication

The fabrication stage begins with the preparation of tools and materials, cutting the aluminum matrix metal into small pieces to be inserted into a ceramic crucible, and preparing sea sand reinforcement particles by pounding and sieving them using a 150 mesh before the electroless coating process. In the electroless coating process, 40 ml of 68% HNO_3

solution was heated to 80°C, then 20 grams of sea sand, 0.5 grams of Al fine powder, and 0.1 grams of Mg fine powder were added. The materials were mixed using a magnetic stirrer and heated for 40 minutes at 100°C. After that, the materials were transferred to a mortar and put into a furnace for 60 minutes at 200°C for drying, followed by 400°C for 120 minutes for the oxidation process, then cooled at room temperature [3].

The next stage is casting using the stir casting method. Stir casting apparatus presented in Figure 1. The aluminum matrix metal is melted in the ceramic crucible at 750°C for 4 hours. After melting, the procedure of stir casting is executed. Sea sand reinforcement particles that have undergone electroless coating are heated at 500°C and added to the molten metal according to the specified weight fraction, along with 1% by weight of Mg powder. Stirring was done with a four-blade impeller at half of the molten metal height for 10 minutes at 600 rpm. After the stir casting process was completed, casting was carried out by heating the permanent mold in a furnace to 500°C. The molten metal is then poured into the mold and allowed to stand for 60 minutes until it hardens into an ingot. After the metal hardens, surface defects are checked. If defects are found, re-casting is done. Otherwise, the machining process can be carried out to obtain the result. The flowchart methodology is presented in Figure 2.

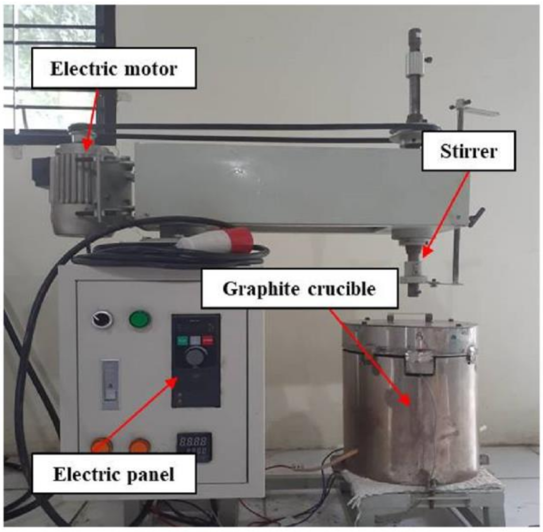

Figure 1. **Stir casting apparatus**

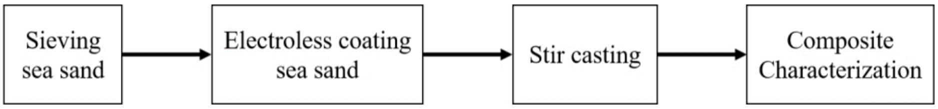

Figure 2. **Flowchart methodology**

3-3- Composite Characterization

Specimen testing was carried out by density testing, specimen microstructure observation, and corrosion rate testing.

- ***Density Testing***

Density testing was carried out using the Archimedes method. The tool used in this study is Vibra Shinko Denshi, Model RJ-320, Japan. Vibra scales are used to measure the density and porosity of the composite. The data obtained from testing the density of a material is the mass in the air and the mass of the object when in water. After obtaining the density in the air and in the water, the data will be processed, to determine the actual density of composite is using Equation 1.

$$\rho\alpha = \frac{ms}{ms-mg} \times \rho H_2O \tag{1}$$

- ***Corrosion Rate Testing***

Tests were conducted to determine the corrosion rate of specimens using the three-electrode cell method. The electrochemical potentiostat machine used in this study is an electrochemical potentiostat with the Corrtest, Model CS350M EIS Potentiostat /Galvanostat, China which has specifications: potential control range: ±10V, potential control accuracy: 0.1%×full range ±1mV, potential resolution: 10µV (>100Hz), 3µV (<10Hz), rise time: <1µS (<10mA), <10µS (<2A), current range: 2nA~2A, 10 ranges, maximum current output: 2A, current control range: ±2A, current control accuracy: 0.1%×full range, current sensitivity: 1pA, reference electrode input impedance: 1012Ω||20pF, compliance voltage: ±21V, CV and LSV scan rate: 0.001mV~10,000V/s. For a picture of the electrochemical potentiostat machine used in this study can be seen in Figure 3.

Figure 3. **Electrochemical potentiostat machine**

Corrosion rate testing was carried out by the potentiodynamic method using an electrochemical potentiostat machine to find the i_{corr} from Tafel diagram [32]. The solution used in this study used 3.5% NaCl. Calculations were carried out using Equation 3 to find corrosion rate.

$$Corrosion\ Rate\ (mmpy) = \frac{K \times icorr \times EW}{\rho} \tag{2}$$

- ***Microstructure Observation***

The data from the potentiodynamic polarisation test was confirmed by micro testing of the sample through the calculation of the volume fraction of the α phase composition and pitting of the corrosion layer using a point counting approach referring to the ASTM E562-11 standard using a grid size of P$\mathcal{T}$ 100-point square pattern [33]. Calculation of volume fraction using point counting is done according to Equation 3.

$$Pp(\alpha) \ = \frac{\sum P\alpha}{P\tau} \times 100 \qquad\qquad Pp(c) \ = \frac{\sum Pc}{P\tau} \times 100 \tag{3}$$

4- Results and Discussion

4-1- Density and Porosity

Density testing was carried out to determine the effect of variations in the addition of weight fractions on the density of AMC, with variations in the weight fraction of sea sand of 2 wt%, 4 wt%, and 6 wt%. Density results are used as parameters in corrosion rate testing using an electrochemical potentiostat machine. The density test results of specimens P20, P21, and P22 can be seen in Figure 4.

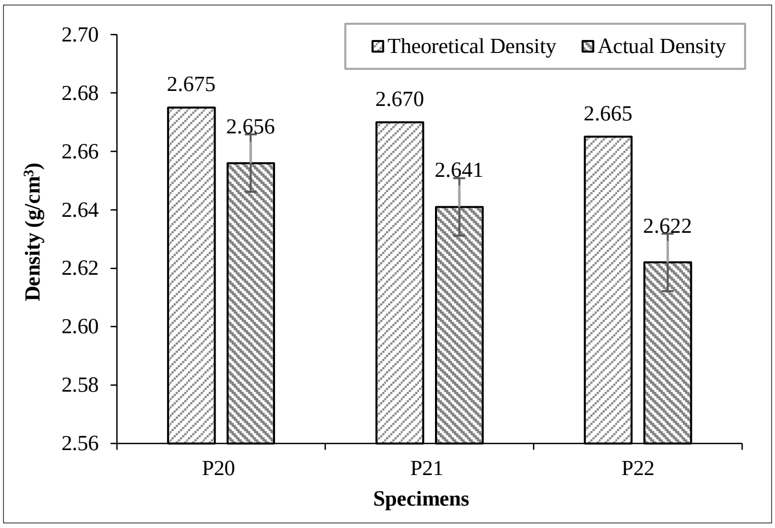

Figure 4. **Density of Al6061-sea sand composite**

Figure 4 shows that the actual density of all variations is lower than the theoretical density due to the presence of voids (porosity) in the composites which are ignored in the theoretical calculations. These voids reduce the actual density compared to the theoretical density. Factors such as temperature, pressure, and time during the stir casting process, as well as inhomogeneous particle distribution, also affect the decreasing density [34, 35]. The difference in the theoretical density of each specimen is due to the variation in the weight fraction added. The test results show a decrease in actual density as the weight fraction of sea sand increases. Specimen P20 with 2 wt% of sea sand added has the highest density of 2.656 g/cm³, while specimens P21 (4 wt%) and P22 (6 wt%) have densities of 2.640 g/cm³ and 2.622 g/cm³ respectively. The addition of sea sand fraction makes the composite lighter because the density of sea sand (2.62 g/cm³) is lower than that of aluminium [34].

The difference between the actual and theoretical densities is caused by the porosity, which increases with the addition of the weight fraction of sea sand. The composite density of each specimen is used to determine the percentage porosity of the material, which is calculated based on the ratio between the composite density and the theoretical density as in Equation 1. The results of the porosity percentage calculation are shown in Figure 5.

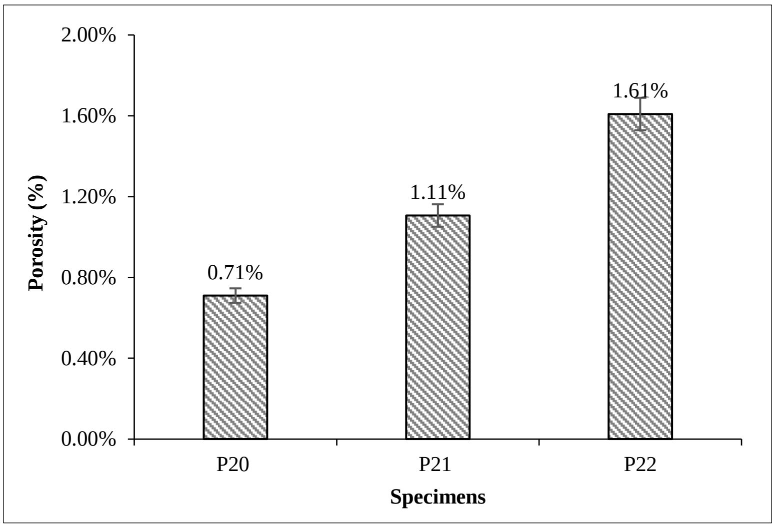

Figure 5. **Porosity of Al6061-sea sand composite**

The test results show that porosity increases with the addition of the weight fraction of sea sand. Specimen P20 with 2 wt% of sea sand had the lowest porosity of 0.71%. The porosity increased in specimen P21 (4 wt%) to 1.11% and reached its peak in specimen P22 (6 wt%) with a porosity of 1.61%. The porosity of the composite increases in response to the addition of reinforcing particles and decreases with increasing density; the higher the density, the lower the porosity. Porosity is caused by gas trapped during stirring and shrinkage during solidification. Decreasing density and increase in porosity are the effect of the mount up of sea sand and molten aluminum reactivity, increasing the chance of porosity due to the weak interfacial bonding [35, 36]. Porosity in particle reinforced composite manufacturing often occurs due to the lack of dispersion of liquid metal into the reinforcing particles. This can be minimized by electroless coating treatment which produces the Al_2MgO_4 spinel phase which has a lower surface tension, so that liquid aluminum can be dispersed on the surface of the liquid metal [37].

4-2- Corrosion Rate

Corrosion rate testing aims to determine the effect of variations in the addition of weight fractions on the corrosion rate of Al 6061-sea sand material. The addition of weight fraction also affects the corrosion resistance of aluminum [7]. Tests were conducted on specimens P20, P21, and P22 using the electrochemical potentiodynamic method with a Cortest potentiostat machine type Cs310 and a 3.5%wt NaCl solution. The i_{corr} results were obtained through Tafel diagram after the test. Chemical Equivalent Al 6061 is required as a parameter in corrosion rate testing, calculated using Equation 2. The test results are used to find i_{corr} based on Tafel diagram (Figure 6) and i_{corr} values for each specimen (P20, P21, and P22) are shown in Table 3.

Table 3. **P20, P21, P22 Specimens i_{corr} Value**

Specimens	(Amps/cm^2)
P20	5.5126×10^{-5}
P21	6.6596×10^{-5}
P22	7.0428×10^{-5}

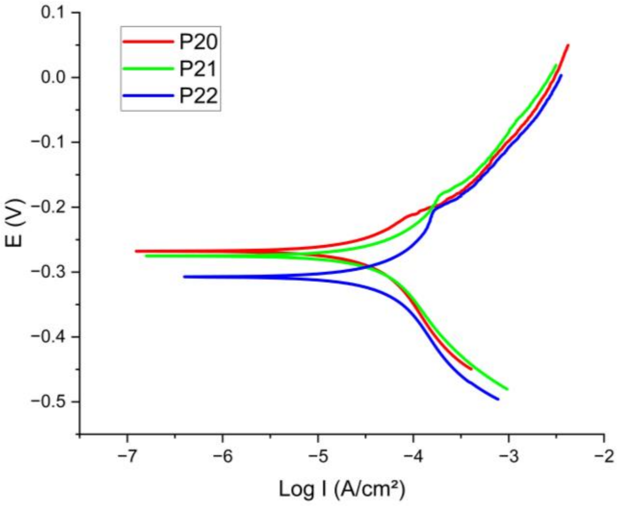

Figure 6. Diagram Tafel

The corrosion rate is gained after calculation using Equation 2, with the parameters i_{corr}, density, and equivalent weight of each specimen. The calculation results show the corrosion rate (mmpy) displayed in Figure 7. Higher i_{corr} values indicate that the corrosion rate occurs faster [22]. Corrosion in aluminum composites is greatly influenced by the interfacial bond between the matrix and the reinforcement particles. If the interfacial bond in the composite is poor, then the gap between the matrix and the reinforcement is the initiation of corrosion. This is in accordance with the study of Prabakaran et al. (2024) which investigated the corrosion behavior between AA6063-SiC-WS_2, which showed that corrosion influenced by the interfacial interaction of the matrix and reinforcement [23]. Generally, particle-reinforced composites experience galvanic corrosion and pitting corrosion when in contact with the environment. In Al6061-sea sand composites, corrosion is formed due to contact between the Al matrix and sea sand particles containing oxides with the NaCl solution. So that Al becomes the cathode and sea sand particles become the cathode. The electrochemical process causes Al to lose electrons that initiate corrosion [21], this is in accordance with a study conducted by Yang, et al., 2024 which investigated the effect of graphite content on corrosion resistance in aluminum matrix composites.

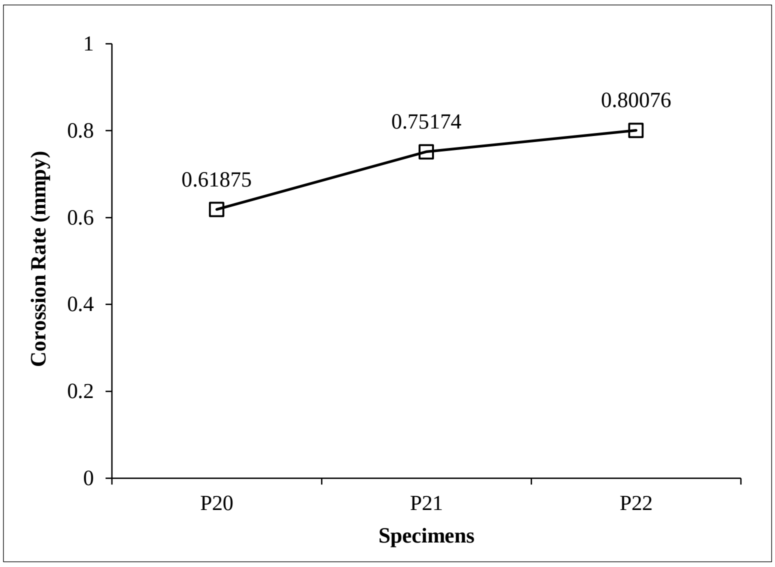

Figure 7. Corrosion rate of specimens P20, P21, and P22

According to the test results, the corrosion rate increases with the addition of the sea sand weight fraction. Figure 7 shows the corrosion rate of specimens P20, P21, and P22. Specimen P20 with 2 wt% of sea sand has the lowest corrosion rate, which is 0.61875 mmpy. Specimen P21 with 4 wt% of sea sand had an increase in corrosion rate to 0.75174 mmpy, and specimen P22 with 6 wt% of sea sand had the highest corrosion rate, which was 0.80076 mmpy. These results show that increasing the weight fraction of sea sand is directly proportional to the increase in corrosion rate. Figure 7 shows that the corrosion product layer is getting bigger with the addition of sea sand reinforcement particles. This shows that the interfacial bond between the reinforcement particles and the matrix is weak. The increase in porosity indicates that the more particles added increases the porosity. The high porosity is related to the faster corrosion rate that occurs due to the weak interfacial bond [23].

Increasing the weight fraction of sea sand in the Al 6061-sea sand composite significantly linear with the corrosion rate increased. This is due to the Fe_2O_3 content in the sea sand acting as a corrosion catalyst and an increase in the electrochemical reaction between the aluminum matrix and the sea sand particles [25]. The potential difference causes the aluminum matrix to become an anode, accelerating galvanic corrosion [38]. In addition, interface defect on the composite surface between the matrix and reinforcement particles allow corrosive ions to enter and accelerate corrosion. Therefore, the corrosion rate increases due to electrochemical reactions, and interface defects [39, 40].

4-3- Microstructure Observation

Corrosion Material micro testing was conducted to observe the microstructure of specimens P20, P21, and P22, both before and after corrosion rate testing, using an optical microscope. The results of metallographic observations are shown in Figure 8.

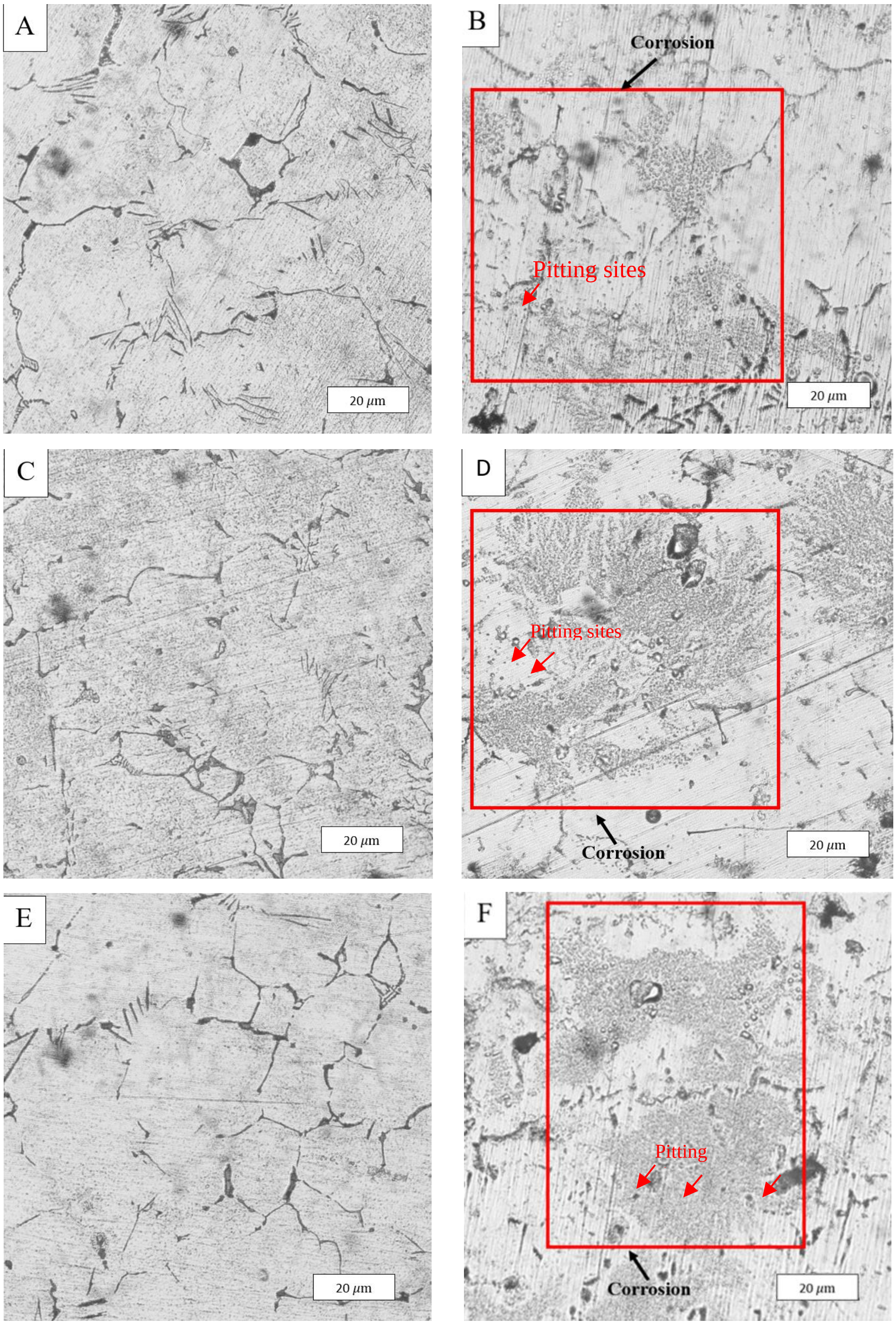

Figure 8. **Microstructure observation Al6061-sea sand a) P20 before corrosion test, b) P20 after corrosion test, c) P21 before corrosion test, d) P21 after corrosion test, e) P22 before corrosion test, and f) P22 after corrosion test**

Figure 8 shows the microstructure of the Al 6061-Sea sand composite before and after corrosion testing using the electrochemical potentiodynamic method. The corrosion test was carried out with a Cortest potentiostat machine type Cs310 and a solution of 3.5%wt NaCl. In specimen P20 with 2 wt% sea sand after the corrosion test, there is an uneven distribution of corrosion. Specimen P21 with 4 wt% of sea sand showed a more even distribution of corrosion than P20. Specimen P22 with 6 wt% of sea sand shows the most even distribution of corrosion compared to other variations.

Based on Figure 9, there are differences in the microstructure and composition of the corrosion product layer between specimens with low and high corrosion rates. Specimen P20 has the lowest corrosion rate (0.61875 mmpy) with few of corrosion product layers (23%) and dominant α Al 6061-Sea sand (77%). An increase in corrosion rate was seen in specimen P21 (0.75174 mmpy) with a layer of corrosion products (35.5%) and α Al 6061-Sea sand (64.5%). Specimen P22 has the highest corrosion rate (0.80076 mmpy) with more corrosion product layers (42%) and dominance of α Al 6061-Sea sand (58%). The changes in microstructure and composition of the corrosion product layers reflect the differences in corrosion rates between specimens.

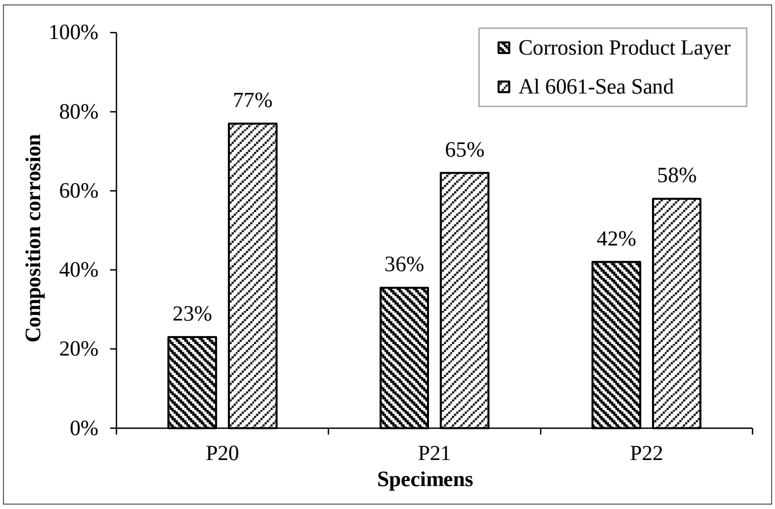

Figure 9. **Composition corrosion product layer**

Figure 9 shows that the corrosion product layer is getting bigger with the addition of sea sand reinforcement particles. This shows that the interfacial bond between the reinforcement particles and the matrix is weak. The increase in porosity indicates that the more particles added increases the porosity. The high porosity is related to the faster corrosion rate that occurs due to the weak interfacial bond. The addition of sea sand weight fraction affects the corrosion rate by triggering galvanic corrosion through electrochemical reaction between the aluminium matrix and sea sand particles [10, 20].

5- Conclusion

The purpose of this study is to analyze the effect of the addition of sea sand on the density and corrosion rate of Al6061 composites fabricated by the stir casting method with variations of the addition of 2 wt%, 4 wt%, and 6 wt%. Since the density of sea sand (2.62 g/cm³) is lower than that of Al6061, there is a decrease in the true density of the composite as the weight fraction of sea sand increases. The percentage of porosity is evaluated by comparing the actual and theoretical densities, which shows a positive correlation between the percentage of sea sand and the porosity value caused by gas entrapment during the manufacturing process. The results of corrosion rate testing using electrochemical potentiodynamic techniques show an increase in corrosion rate as the concentration of sea sand increases. The measured corrosion rate values for the addition of 2wt%, 4wt%, and 6wt% sea sand are 0.61875 mmpy, 0.75174 mmpy, and 0.80076 mmpy, respectively. This phenomenon is attributed to the presence of Fe_2O_3 in the sea sand, which acts as a corrosion catalyst. In addition, the strength of the interfacial bonding between the Al6061 matrix and the sea sand particles has a significant effect on the corrosion susceptibility. Weak interfacial bonding facilitates the initiation of corrosion at the grain boundaries. Microstructural analysis was performed to validate the results of the corrosion rate test using the electrochemical potentiodynamic method, which showed an increase in the formation of corrosion products and a more uniform distribution with increasing sea sand concentration, supporting the results of the corrosion rate test.

6- Declarations

6-1- Author Contributions

Conceptualization, E.S. and H.I.A.; methodology, T.T. and R.M.A.; validation, T., H.I.A., and W.W.R.; formal analysis, R.M.A. and G.P.; investigation, I.H; G.P., and H.S.; writing—original draft preparation, F.M.M, H.I.A., and G.P.; writing—review and editing, F.M.M, H.I.A., and G.P.; visualization, T.; supervision, E.S. and H.S.; funding acquisition, E.S. All authors have read and agreed to the published version of the manuscript.

6-2- Data Availability Statement

Data sharing is not applicable to this article.

6-3- Funding and Acknowledgements

This research is funded by the Directorate of Research, Technology and Community Service, Directorate General of Higher Education, Research and Technology, Ministry of Education, Culture, Research and Technology of the Republic of Indonesia through the Fundamental Research scheme with contract number 086/E5/PG.02.00.PL/2024 and 1076.1/UN27.22/PT.01.03/2024.

6-4- Institutional Review Board Statement

Not applicable.

6-5- Informed Consent Statement

Not applicable.

6-6- Conflicts of Interest

The authors declare that there is no conflict of interest regarding the publication of this manuscript. In addition, the ethical issues, including plagiarism, informed consent, misconduct, data fabrication and/or falsification, double publication and/or submission, and redundancies have been completely observed by the authors.

7- References

[1] Griffiths, A. J., & Turnbull, A. (1994). An investigation of the electrochemical polarisation behaviour of 6061 aluminium metal matrix composites. Corrosion Science, 36(1), 23–35. doi:10.1016/0010-938X(94)90106-6.

[2] Sijo, M. T., & Jayadevan, K. R. (2016). Analysis of Stir Cast Aluminium Silicon Carbide Metal Matrix Composite: A Comprehensive Review. Procedia Technology, 24, 379–385. doi:10.1016/j.protcy.2016.05.052.

[3] Zulfia, A., & Adyatma, A. I. (2013). Electroless plating of Al2O3 particles reinforced composites. Advanced Materials Research, 789, 66–71. doi:10.4028/www.scientific.net/AMR.789.66.

[4] Laima, L., Xiaoyue, T., Zelong, L., Guangnan, L., Xiang, Z., Jigui, C., & Yucheng, W. (2015). Preparation and Properties of W-15Cu Composite by Electroless Plating and Powder Metallurgy. Rare Metal Materials and Engineering, 44(12), 3005–3008. doi:10.1016/s1875-5372(16)60039-5.

[5] Siddesh Kumar, N. M., Sadashiva, M., Monica, J., & Praveen Kumar, S. (2022). Investigation on Corrosion Behaviour of Hybrid Aluminium Metal Matrix Composite Welded by Friction Stir Welding. Materials Today: Proceedings, 52, 2339–2344. doi:10.1016/j.matpr.2022.01.362.

[6] Verma, A. S., Sumankant, Suri, N. M., & Yashpal. (2015). Corrosion Behavior of Aluminum Base Particulate Metal Matrix Composites: A Review. Materials Today: Proceedings, 2(4–5), 2840–2851. doi:10.1016/j.matpr.2015.07.299.

[7] Samuel Ratna Kumar, P. S., Robinson Smart, D. S., & John Alexis, S. (2017). Corrosion behaviour of Aluminium Metal Matrix reinforced with Multi-wall Carbon Nanotube. Journal of Asian Ceramic Societies, 5(1), 71–75. doi:10.1016/j.jascer.2017.01.004.

[8] Paciej, R. C., & Agarwala, V. S. (1986). Metallurgical Variables Influencing the Corrosion Susceptibility of a Powder Metallurgy Sicw/Al Composite. Corrosion, 42(12), 718–729. doi:10.5006/1.3583046.

[9] Ashok Kumar, R., Akash, S. J., Arunkumar, S., Balaji, V., Balamurugan, M., & Jeevan Kumar, A. (2020). Fabrication and Corrosion Behaviour of Aluminium Metal Matrix Composites - A Review. IOP Conference Series: Materials Science and Engineering, 923(1), 012056. doi:10.1088/1757-899X/923/1/012056.

[10] Han, Y. M., & Chen, X. G. (2015). Electrochemical behavior of Al-B4C metal matrix composites in NaCl solution. Materials, 8(9), 6455–6470. doi:10.3390/ma8095314.

[11] Das, S. (2010). Effect of particle size and amount on corrosion behaviour of Al-4·5 wt-%Cu/zircon sand composite. Corrosion Engineering Science and Technology, 45(1), 94–96. doi:10.1179/147842209X12464471864411.

[12] Trowsdale, A. J., Noble, B., Harris, S. J., Gibbins, I. S. R., Thompson, G. E., & Wood, G. C. (1996). The influence of silicon carbide reinforcement on the pitting behaviour of aluminium. Corrosion Science, 38(2), 177–191. doi:10.1016/0010-938X(96)00098-4.

[13] Zhang, S. D., Zhang, W. L., Wang, S. G., Gu, X. J., & Wang, J. Q. (2015). Characterisation of three-dimensional porosity in an Fe-based amorphous coating and its correlation with corrosion behaviour. Corrosion Science, 93, 211–221. doi:10.1016/j.corsci.2015.01.022.

[14] Cheng, Y. L., Chen, Z. H., Wu, H. L., & Wang, H. M. (2007). The corrosion behaviour of the aluminum alloy 7075/SiCp metal matrix composite prepared by spray deposition. Materials and Corrosion, 58(4), 280–284. doi:10.1002/maco.200604003.

[15] Alaneme, K. K., & Bodunrin, M. O. (2011). Corrosion Behavior of Alumina Reinforced Aluminium (6063) Metal Matrix Composites. Journal of Minerals and Materials Characterization and Engineering, 10(12), 1153–1165. doi:10.4236/jmmce.2011.1012088.

[16] Nunes, P. C. R., & Ramanathan, L. V. (1995). Corrosion behavior of alumina-aluminum and silicon carbide-aluminum metal-matrix composites. Corrosion, 51(8), 610–617. doi:10.5006/1.3293621.

[17] Zhu, J., & Hihara, L. H. (2010). Corrosion of continuous alumina-fibre reinforced Al-2 wt.% Cu-T6 metal-matrix composite in 3.15 wt.% NaCl solution. Corrosion Science, 52(2), 406–415. doi:10.1016/j.corsci.2009.09.028.

[18] Aliyu, I., Sapuan, S. M., Zainudin, E. S., Zuhri, M. Y. M., & Ridwan, Y. (2023). Hardness and corrosion behaviour of stir cast LM26 Al/sugar palm fibre ash composites. Multidiscipline Modeling in Materials and Structures, 19(4), 748–765. doi:10.1108/MMMS-10-2022-0219.

[19] Fayomi, O. S. I., Anawe, P. A. L., & Daniyan, A. (2018). The Impact of Drugs as Corrosion Inhibitors on Aluminum Alloy in Coastal-Acidified Medium. Corrosion Inhibitors, Principles and Recent Applications, IntechOpen, London, United Kingdom. doi:10.5772/intechopen.72942.

[20] Kosari, A., Tichelaar, F., Visser, P., Zandbergen, H., Terryn, H., & Mol, J. M. C. (2020). Dealloying-driven local corrosion by intermetallic constituent particles and dispersoids in aerospace aluminium alloys. Corrosion Science, 177, 108947. doi:10.1016/j.corsci.2020.108947.

[21] Yang, S., Gao, X., Li, W., Dai, Y., Zhang, J., Zhang, X., & Yue, H. (2024). Effects of the graphene content on mechanical properties and corrosion resistance of aluminum matrix composite. Journal of Materials Research and Technology, 28, 1900–1906. doi:10.1016/j.jmrt.2023.12.059.

[22] Chen, S., Niu, P., Huang, Y., Li, Y., Fu, X., Ke, L., Liu, F., & Liu, F. (2025). Corrosion properties and mechanisms of friction stir lap welded TiB2/2024 aluminum matrix composite joint. Electrochimica Acta, 509, 1–12. doi:10.1016/j.electacta.2024.145306.

[23] Prabakaran, V., R, P., M, P., & S, K. kumar. (2024). Study of tribological performance and corrosion resistance of aluminum alloy 6063 composites enhanced with a combination of silicon carbide and tungsten disulfide particles. Results in Surfaces and Interfaces, 15, 100233. doi:10.1016/j.rsurfi.2024.100233.

[24] Patel, M., Jain, S., & Murugesan, J. (2025). Investigation of Mechanical Properties, Fretting Wear, and Corrosion Behaviour of AA6063/Si3N4 Nanocomposites Fabricated via Friction Stir Processing. Arabian Journal for Science and Engineering, 50(17), 13795–13805. doi:10.1007/s13369-024-09551-z.

[25] Cui, S., Tong, W., Zhai, H., Zhang, J., Xiong, D., Liu, J., & Qiang, Y. (2025). Corrosion and wear behavior of the Fe-based amorphous coating in extremely aggressive solutions. Intermetallics, 181. doi:10.1016/j.intermet.2025.108713.

[26] Kiourtsidis, G. E., & Skolianos, S. M. (2007). Pitting corrosion of artificially aged T6 AA2024/SiCp composites in 3.5 wt.% NaCl aqueous solution. Corrosion Science, 49(6), 2711–2725. doi:10.1016/j.corsci.2006.10.008.

[27] An, Q., Cong, X., Shen, P., & Jiang, Q. (2019). Roles of alloying elements in wetting of SiC by Al. Journal of Alloys and Compounds, 784, 1212–1220. doi:10.1016/j.jallcom.2019.01.138.

[28] Zakaulla, M., Khan, A. R. A., & Mukunda, P. G. (2014). Effect of Electroless Copper Coating on the Corrosion Behavior of Aluminium Based Metal Matrix Composites Reinforced with Silicon Carbide Particles. Journal of Minerals and Materials Characterization and Engineering, 02(01), 21–25. doi:10.4236/jmmce.2014.21004.

[29] Gehre, P., Aneziris, C. G., Berek, H., Parr, C., & Reinmöller, M. (2015). Corrosion of magnesium aluminate spinel-rich refractories by sulphur-containing slag. Journal of the European Ceramic Society, 35(5), 1613–1620. doi:10.1016/j.jeurceramsoc.2014.11.031.

[30] Hidayat, T. A. S., Surojo, E., Ariawan, D., Akbar, H. I., Imanullah, F., & Fanani, E. W. A. (2024). Experimental Study of Quenching Agent on AA6061-Sea Sand Composite: Effect Quenching Medium to Mechanical Properties and Distortion. Evergreen, 11(3), 2273–2283. doi:10.5109/7236870.

[31] Mufti, H. R., Akbar, H. I., Surojo, E., Wibowo, W., Triyono, T., Cahyono, S. I., Muhayat, N., & Triyono, T. (2021). The Effect of Cooling Media on T6 Heat Treatment on the Tensile Strength and Microstructure of Al6061-Beach Sand Composites. METAL: Jurnal Sistem Mekanik Dan Termal, 5(2), 51–59. doi:10.25077/metal.5.2.51-59.2021.

[32] Jebaraj, A. V., Aditya, K. V. V., Kumar, T. S., Ajaykumar, L., & Deepak, C. R. (2019). Mechanical and corrosion behaviour of aluminum alloy 5083 and its weldment for marine applications. Materials Today: Proceedings, 22, 1470–1478. doi:10.1016/j.matpr.2020.01.505.

[33] ASTM E562-11. (2019). Standard Test Method for Determining Volume Fraction by Systematic Manual Point Count. ASTM International, Pennsylvania, United States. doi:10.1520/E0562-11.

[34] Sulardjaka, S., Nugroho, S., & Wacono, D. D. (2015). The Effect of Percentage Weight of Sic Powder on the Hardness and Bending Strength of Composites with Alsitib Matrix Reinforced by Sic Powder. Rotasi, 17(3), 156. doi:10.14710/rotasi.17.3.156-161.

[35] Hashim, J., Looney, L., & Hashmi, M. S. J. (1999). Metal matrix composites: production by the stir casting method. Journal of Materials Processing Technology, 92–93, 1–7. doi:10.1016/s0924-0136(99)00118-1.

[36] Garg, P., Jamwal, A., Kumar, D., Sadasivuni, K. K., Hussain, C. M., & Gupta, P. (2019). Advance research progresses in aluminium matrix composites: manufacturing & applications. Journal of Materials Research and Technology, 8(5), 4924–4939. doi:10.1016/j.jmrt.2019.06.028.

[37] Zheng, J., Shu, G., Wang, W., Li, Q., & Liu, W. (2015). Surface quality improvement of B 4 C particles for electroless copper coating by Cu activation and oxidation roughening methods. Applied Surface Science, 349, 733–739. doi:10.1016/j.apsusc.2015.05.052.

[38] Abbass, M. K., Hassan, K. S., & Alwan, A. S. (2015). Study of Corrosion Resistance of Aluminum Alloy 6061/SiC Composites in 3.5% NaCl Solution. International Journal of Materials, Mechanics and Manufacturing, 3(1), 31–35. doi:10.7763/ijmmm.2015.v3.161.

[39] Reena Kumari, P. D., Nayak, J., & Nityananda Shetty, A. (2016). Corrosion behavior of 6061/Al-15 vol. pct. SiC(p) composite and the base alloy in sodium hydroxide solution. Arabian Journal of Chemistry, 9, S1144–S1154. doi:10.1016/j.arabjc.2011.12.003.

[40] Kumar, S. R., Krishnaa, S. D., Krishna, M. D., Gokulkumar, N. T., & Akilesh, A. R. (2021). Investigation on corrosion behaviour of aluminium 6061-T6 alloy in acidic, alkaline and salt medium. Materials Today: Proceedings, 45, 1878–1881. doi:10.1016/j.matpr.2020.09.079.